The Astrophysical Journal, 643: L25–L28, 2006 May 20

DETECTION OF ACETAMIDE (CH_3CONH_2): THE LARGEST INTERSTELLAR MOLECULE WITH A PEPTIDE BOND

J. M. Hollis,[1] F. J. Lovas,[2] Anthony J. Remijan,[3] P. R. Jewell,[3] V. V. Ilyushin,[4] and I. Kleiner[5]

Received 2006 March 7; accepted 2006 April 14; published 2006 May 2

ABSTRACT

Acetamide (CH_3CONH_2) has been detected in emission and absorption toward the star-forming region Sagittarius B2(N) with the 100 m Green Bank Telescope (GBT) by means of four *A*-species and four *E*-species rotational transitions. All transitions have energy levels less than 10 K. The Sgr B2(N) cloud is known to have a cold halo with clumps of gas at several different velocities. Absorption features are largely characterized by local standard of rest (LSR) velocities that are typical of the two star-forming cores with systemic LSR velocities of +64 and +82 km s^{-1}. Continuum sources embedded within the star-forming cores give rise to the absorption from the molecular gas halo surrounding the cores. Emission features are seen at an approximate intermediate LSR velocity of +73 km s^{-1} that characterizes the widespread molecular halo that has a spatial scale of a few arcminutes. Two low-energy transitions of formamide ($HCONH_2$) were also observed with the GBT toward Sagittarius B2(N) since formamide is the potential parent molecule of acetamide; both molecules are the only interstellar species with an NH_2 group bound to a CO group, the so-called peptide bond, that provides the linkage for the polymerization of amino acids. While the acetamide transitions observed appear to be confined to the cold (~8 K) halo region, only the 1_{01}–0_{00} transition of formamide appears to be exclusively from the cold halo; the 3_{12}–3_{13} transition of formamide is apparently contaminated with emission from the two hot cores. The relative abundance ratio of acetamide to formamide is estimated to be in the range of ~0.1 to ~0.5 in the cold halo. The exothermic neutral-radical reaction of formamide with methylene (CH_2) may account for the synthesis of interstellar acetamide in the presence of shock phenomenon in this star-forming region.

Subject headings: ISM: abundances — ISM: clouds — ISM: individual (Sagittarius B2(N-LMH)) — ISM: molecules — radio lines: ISM

1. INTRODUCTION

Ultraviolet photolysis and proton irradiation of realistic cometary ice analogs easily produce simple organic molecules, such as carbon dioxide (CO_2), the formyl radical (HCO), and formaldehyde (H_2CO), and moderately more complex organic species, such as ethanol (CH_3CH_2OH), formamide ($HCONH_2$), and acetamide (CH_3CONH_2), as well as larger species (Allamandola et al. 1999; see also Fig. 4 of Hudson et al. 2001). While comets may contain most if not all of these species formed in such laboratory experiments, neither formamide nor acetamide has yet been reported in comets. Encouraged by the results of cometary ice analog laboratory experiments, and the fact that six-atom formamide has been long established as an interstellar species (Rubin et al. 1971) and could be the parent molecule, we conducted an interstellar search for nine-atom acetamide. These observations test whether this moderately complex species can be traced back to molecular formation in interstellar clouds from which protoplanetary systems and comets themselves form.

Rotational spectra of acetamide are complicated by the internal rotation of the methyl group (see Fig. 1). An ~25 cm^{-1} barrier to rotation of the methyl group gives rise to torsional structure in the ground and excited torsional states. In this work we have only sought transitions of the ground torsional state. The ^{14}N nucleus causes the hyperfine splitting (hfs) observed in the laboratory. For convenience, the transition labeling convention $J'_{K\_K_+}$–$J''_{K\_K_+}$ *A*-species (or *E*-species) is adopted here, where *A* and *E* are used in place of the equivalent parity sign convention employed in the most recent spectroscopic work on acetamide (Suenram et al. 2001; Ilyushin et al. 2004). A discussion of acetamide transition notation conventions used in spectroscopic literature can be found in Suenram et al. (2001) and Ilyushin et al. (2004).

2. OBSERVATIONS AND RESULTS

Spectral line observations of acetamide and formamide were conducted with the NRAO[6] 100 m Robert C. Byrd Green Bank Telescope (GBT) in accordance with Table 1, which lists the receiver band, receiver tuning range, number of intermediate frequencies (IFs) employed, number of polarizations per IF, bandwidth per IF, spectrometer channel spacing, pointing source used, and observational date in the eight columns. Table 2 lists the rotational transitions of the molecules sought. The transition quantum numbers, the calculated transition rest frequency, the product of the square of the dipole moment (μ^2) and transition line strength (*S*), the energy of the lower level (E_l), the telescope beamwidth (θ_B), and the telescope beam efficiency (η_B) are listed in the first six columns. For acetamide, the *A*- and *E*-species were considered separately, and therefore the energies given in Table 2 column (4) are relative to the lowest *A*- or *E*-species level. Antenna temperatures are on the T_A^* scale (Ulich & Haas 1976) with estimated 20% uncertainties. GBT half-power beamwidths can be approximated by θ_B =

[1] NASA Goddard Space Flight Center, Computational and Information Sciences and Technology Office, Code 606, Greenbelt, MD 20771.

[2] Optical Technology Division, National Institute of Standards and Technology, Gaithersburg, MD 20899.

[3] National Radio Astronomy Observatory, 520 Edgemont Road, Charlottesville, VA 22903-2475.

[4] Institute of Radio Astronomy of the National Academy of Sciences of Ukraine (NASU), Chervonopraporna 4, 61002 Kharkov, Ukraine.

[5] Laboratoire Inter-Universitaire des Systémes Atmosphériques (LISA), CNRS, Université Paris 12 et Paris 7, 61 avenue Général de Gaulle, 94010 Créteil Cédex France.

[6] The National Radio Astronomy Observatory is a facility of the National Science Foundation, operated under cooperative agreement by Associated Universities, Inc.

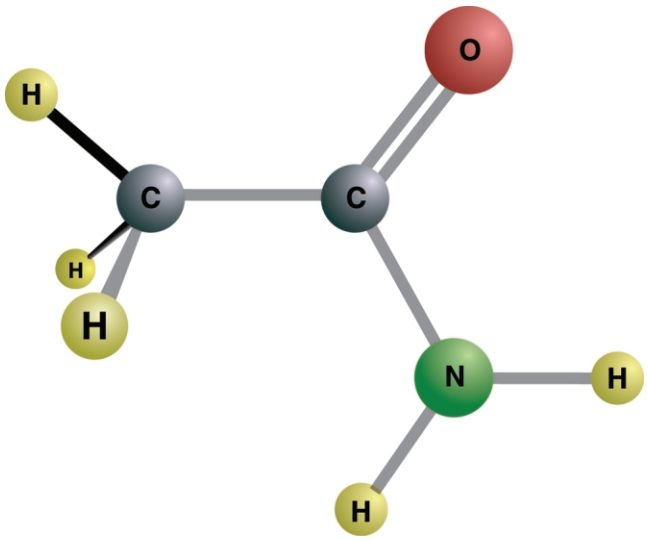

FIG. 1.—Schmatic diagram showing the molecular structure of acetamide.

740″/ν(GHz). The Sgr B2(N-LMH) J2000 pointing position employed was $\alpha = 17^{h}47^{m}19\overset{s}{.}8$, $\delta = -28°22'17''$, and an LSR source velocity of +64 km s^{-1} was assumed. Data were taken in the OFF-ON position-switching mode, with the OFF position 60′ east in azimuth with respect to the ON-source position. A single scan consisted of 2 minutes in the OFF followed by 2 minutes in the ON. The two polarization outputs from the spectrometer were averaged in the final data reduction process to improve the signal-to-noise ratio.

Spectra of formamide and acetamide are shown in Figures 2 and 3, respectively. Each spectrum was processed with a median filter to remove instrumental slopes in the bandpass; this effectively removes the source continuum level. The data in Figures 2 and 3 are summarized in Table 2, in which column (7) gives an estimate of the integrated intensity of each line complex and uncertainty estimate obtained from the sum of fitting multiple Gaussians. The average source continuum level removed by the median filter process appears in column (8). The continuum level of each OFF-ON scan was observed to vary with a standard deviation of ~0.4 K with respect to the average because of fluctuations in atmospheric and receiver system stability. By inspection, the ratio of individual line intensities in Figures 2 and 3 to corresponding source continuum temperatures in Table 2 column (8) indicates that the apparent optical depths of the lines are much less than 1, consistent with the optically thin case.

At frequencies less than 50 GHz, the GBT samples the spatially extended cold gas that is characterized by a number of large complex molecules that have rotational transitions occurring between low-energy levels. For example, GBT observations of low-energy transitions of glycolaldehyde (CH_2OHCHO), ethylene glycol ($HOCH_2CH_2OH$), propenal (CH_2CHCHO), and propanal (CH_3CH_2CHO) are indicative of widespread spatial distributions on the order of a few arcminutes toward Sgr B2(N) (see Hollis et al. 2004a, 2004b, Hollis 2005, and references therein), and, in particular, low-energy transitions of glycolaldehyde are characterized by a state temperature of ~8 K (Hollis et al. 2004a). Furthermore, absorption spectra in low-energy transitions of glycolaldehyde, propenal, propanal, formimide, and acetamide all look very similar with principal absorption components at LSR velocities of +64 and +82 km s^{-1} that are characteristic of the two Sgr B2(N) star-forming cores with these systemic LSR velocities (Mehringer & Menten 1997); when present, emission spectra for these species tend to be centered at a median LSR velocity of +73 km s^{-1} that is typical of the extended halo around the two cores.

In a radiative transfer analysis of formamide and acetamide observations, we ignore the possibility of nonthermal excitation and assume that the spatial distribution of the transitions between extremely low energy levels resides in the Sgr B2(N) halo region and therefore fills the telescope beam. To obtain an estimate of the total column density (N_T) of each molecule, we assume that the rotational partition function (Q) can be characterized by a single-state temperature (T_s), and we use the entire line complex integrated line intensity ($W = \int \Delta T_A^*(v)dv$) to mitigate the competing effects of emission and absorption that may be present in each transition to varying degrees.

For emission,

$$N_T = \frac{W}{\eta_B(8\pi^3/3k)\nu\mu^2 S} Qe^{E_u/kT_s}\left(1 - \frac{e^{h\nu/kT_s} - 1}{e^{h\nu/kT_{\rm bg}} - 1}\right)^{-1}. \quad (1)$$

For absorption,

$$N_T = \frac{WQ}{\eta_B(8\pi^3/3h)(T_s - T_c/\eta_B - T_{\rm bg})\mu^2 S(e^{-E_l/kT_s} - e^{-E_u/kT_s})}. \quad (2)$$

Both equations employ cgs units; $T_{\rm bg} = 2.7$ K; all parameters can be obtained directly or derived from Table 2 parameters (e.g., W, η_B, T_c, E_l, E_u, ν, $\mu^2 S$) with the exception of Q; and T_s cases of 5 and 8 K are evaluated for the cold halo. Since formamide is an asymmetric top, Q can be approximated as $1.87T_s^{1.5}$. From first principles we derive $Q(T_s = 5\ {\rm K}) = Q_A + Q_E = 81.6 + 89.1$ and $Q(T_s = 8\ {\rm K}) = Q_A + Q_E = 164.1 + 179.4$ for acetamide. Calculations for N_T appear in Table 2 columns (9) and (10) for the state temperature cases of 5 and 8 K, respectively.

3. DISCUSSION

Figure 2 shows that the hfs of formamide is only partially resolved because of the conflict with the systemic LSR velocities of the two Sgr B2(N) hot cores. In either T_s case shown

TABLE 1
OBSERVATIONAL PARAMETERS

Band (1)	Receiver (GHz) (2)	IFs (3)	Polarizations (4)	IF Bandwidth (MHz) (5)	Resolution (kHz) (6)	Pointing Source (7)	Dates (8)
X	8–10	4	2	200	24.4	1700−261	2005 Sep 6, 18, 19
Ku	12–15.4	4	2	200	24.4	1700−261	2004 Mar 4
	12–15.4	4	2	200	24.4	1700−261	2005 Sep 7, 14, 22
K	18–22.5	4	2	200	24.4	1700−261	2004 Mar 13, Apr 5, 6, 15
	22–26.5	4	2	200	24.4	1733−130	2005 Apr 1
Q	40–48	4	2	800	390.7	1733−130	2005 Mar 14, 19, 22

TABLE 2
SUMMARY OF OBSERVATIONS TOWARD SGR B2(N-LMH)

Transition ($J'_{K_-K_+}$–$J''_{K_-K_+}$) (1)	Frequency[a] (MHz) (2)	μ^2S[b] (D^2) (3)	E_l (cm^{-1}) (4)	θ_B (arcsec) (5)	η_B (6)	W[c] (K km s^{-1}) (7)	T_c (K) (8)	N_T(5 K)[c] (10^{13} cm^{-2}) (9)	N_T(8 K)[c] (10^{14} cm^{-2}) (10)
Formamide ($HCONH_2$)									
3_{12}–3_{13} $F = 3$–3	9235.119(2)								
3_{12}–3_{13} $F = 4$–4	9237.034(2)	7.62	6.1620	80	0.88	11.5(2)	25.3	867.0(160)	61.6(11)
3_{12}–3_{13} $F = 2$–2	9237.704(2)								
1_{01}–0_{00} $F = 0$–1	21206.450(2)								
1_{01}–0_{00} $F = 2$–1	21207.334(1)	13.08	0.0000	35	0.77	−9.5(2)	7.6	11.3(3)	5.86(12)
1_{01}–0_{00} $F = 1$–1	21207.922(3)								
Acetamide (CH_3CONH_2)									
2_{20}–2_{11} A	9254.418(4)	25.48	1.7968	80	0.88	−1.23(1)	25.3	5.53(11)	1.64(1)
1_{01}–1_{11} E	13388.703(4)	7.93	0.0367	55	0.85	0.31(7)	12.6	22.70(500)	3.10(70)
4_{31}–4_{22} A	14210.349(4)	47.24	6.0014	52	0.84	−0.56(7)	14.6	5.58(70)	1.15(14)
3_{30}–3_{21} A	14441.705(4)	24.98	3.7859	51	0.84	−0.76(3)	11.5	9.98(32)	2.81(11)
2_{02}–2_{12} E	15115.748(4)	14.25	0.9721	49	0.84	0.09(2)	12.3	4.34(90)	0.53(12)
2_{21}–1_{11} E	22095.527(4)	19.68	0.0367	33	0.76	0.19(6)/−0.32(6)	7.2	6.10(132)	1.67(27)
3_{31}–3_{22} A	22769.635(4)	16.40	3.4651	32	0.75	−0.19(3)	6.5	4.53(71)	1.83(29)
4_{23}–3_{31} E	47373.320(2)	41.64	2.0608	16	0.41	−0.29(6)	1.4	10.20(200)	…[d]

[a] Formamide rest frequencies from present work; acetamide rest frequencies from Ilyushin et al. (2004). Uncertainties in parentheses refer to the least significant digit and are 2 σ values (type A coverage $k = 2$) (Taylor & Kuyatt 1994).

[b] Formamide $\mu_a = 3.616(10)$ D (Kurland & Wilson 1957); acetamide $\mu_a = -1.14$ D and $\mu_b = -3.5$ D were derived from Kojima et al. (1987).

[c] Uncertainties are 1 σ values (type A coverage $k = 1$) (Taylor & Kuyatt 1994).

[d] Indeterminate column density for 8 K (see text).

in Table 2, the 1_{01}–0_{00} transition of formamide observed in absorption with $\theta_B \sim 35''$ has a much lower N_T than the 3_{12}–3_{13} transition observed in emission with $\theta_B \sim 80''$. The 3_{12}–3_{13} transition of formamide has energy levels ~10 K higher than the 1_{01}–0_{00} transition, which should sample the cold halo exclusively because its lower energy levels would not be well populated in hot cores that have scale sizes of a few arcseconds. Even though the 3_{12}–3_{13} transition of formamide would obviously suffer beam dilution with respect to the small hot cores, this transition must be contaminated by hot core emission, in order to explain the higher total column densities derived from it. Thus, we conclude that the N_T determined from the 1_{01}–0_{00} transition best represents the abundance of formamide in the cold halo region.

The hfs for each acetamide transition reported here cannot be even partially resolved because of the small splitting calculated from the *eQq* constants reported by Ilyushin et al. (2004) and the broad LSR velocity structure of the two hot cores. Even so, the 2_{20}–2_{11} *A* transition of acetamide in Figure 3 shows some of the influence of its underlying hfs because the strongest absorption feature is slightly offset to the high-frequency side of the +64 km s^{-1} fiducial. Figure 3 transitions show the competing effects of emission and absorption in spectral features at +64, +73, and +82 km s^{-1}, all of which are weak in comparison to the transitions of formamide. In the $T_s = 8$ K case shown in Table 2 for acetamide, the N_T determined for transitions predominantly displaying emission or absorption are quite similar in magnitude; however, the N_T for the 4_{23}–3_{31} *E* transition seen in absorption cannot be computed in this case because an 8 K state temperature is too large for absorption to occur owing to a low source continuum temperature (see eq. [2] and T_c in Table 2). This suggests that a lower state temperature may be appropriate across all acetamide transitions; however, while the 4_{23}–3_{31} *E* transition can now be used to calculate a N_T in the $T_s = 5$ K case, the N_T computed using the 1_{01}–0_{11} *E* transition seen in emission is quite large compared to values obtained from all other transitions. These results are probably symptomatic of assuming a single-state temperature for all the transitions of acetamide. From this exercise, we conclude that the N_T for acetamide in the halo region is better represented by the $T_s = 8$ K case, because of the consistency of values that are obtained by seven of the eight transitions that yield an average $\langle N_T(8\ \mathrm{K})\rangle = 1.8(9) \times 10^{14}$ cm^{-2} and an acetamide-to-formamide abundance ratio of ~0.1 to ~0.5.

Since exothermic neutral-radical reactions have been shown to be efficient at low temperatures (Herbst 1995), the acetamide observed toward Sgr B2(N) may be produced by the exothermic reaction of formamide with the methylene (CH_2) radical:

$$HCONH_2 + CH_2 \rightarrow CH_3CONH_2. \quad (3)$$

Equation (3) may have an activation barrier because electronic spin is not conserved in the reaction, but such a barrier could be overcome by prevalent large- and small-scale shocks in this star-forming region (see Chengalur & Kanekar 2003 and references therein). The mere presence of acetamide and formamide in interstellar clouds suggests that these two species will already be present before comets form. The thermal transients caused by shocks within star-forming regions undoubtedly have similarities to the cometary ices bombarded with UV radiation or proton flux that allow reaction activation barriers to be overcome in laboratory experiments. A comet at the periastron passage would experience maximal UV radiation and the particle wind from a star that has reached the main sequence, and, as a result, processes identical to the laboratory ice analog experiments could efficiently proceed. However, in the dust-shielded environment of dense clouds, where stars are in the process of forming, UV and particle wind sources of energy (see Moore et al. 2001) may be less efficient than shock processing associated with material infall and accretion.

In summary, acetamide has been detected in Sgr B2(N) by means of four *A*-species and four *E*-species transitions that have energy levels less than 10 K. These transitions sample the cold (~8 K) halo that surrounds the star-forming cores with systemic LSR velocities of +64 and +82 km s^{-1}. The 1_{01}–0_{00} transition of formamide was also observed. Formamide is likely the par-

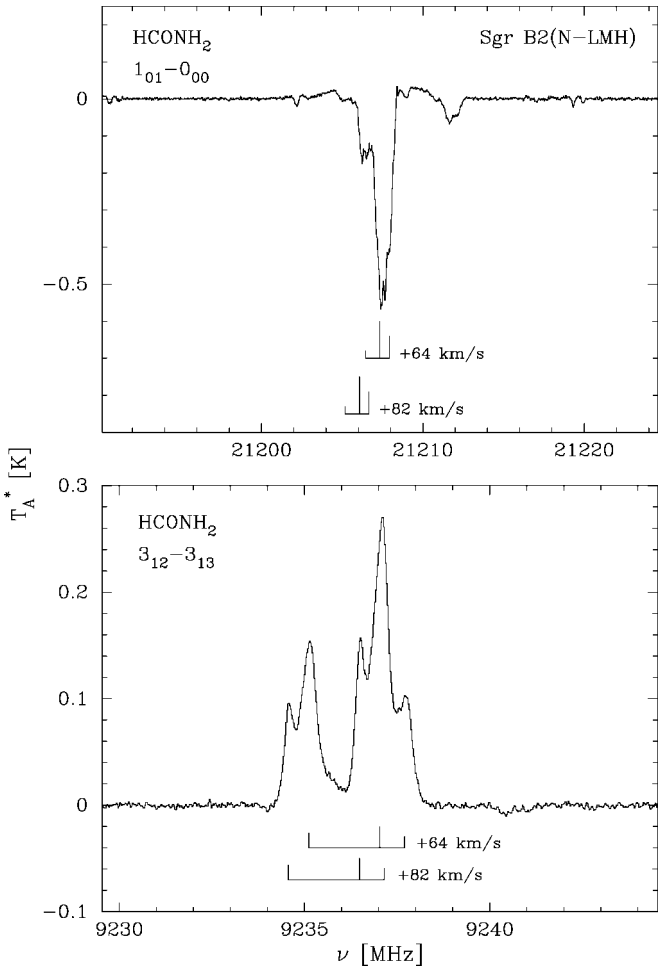

FIG. 2.—Formamide ($HCONH_2$) spectra toward Sgr B2(N-LMH) at 24.4 kHz channel spacing. Transition quantum numbers are shown in each panel. A continuum baseline has been removed (see text). Horizontal frequency axes are based on transition rest frequencies in Table 2 at an assumed LSR source velocity of +64 km s^{-1}. Relative intensities of the partially resolved hyperfine structure are shown where LSR velocities of +64 and +82 km s^{-1} fall on the frequency axis. The prominent absorption feature near 21212 MHz is due to formamide in the +3 km s^{-1} LSR velocity spiral arm cloud along the line of sight.

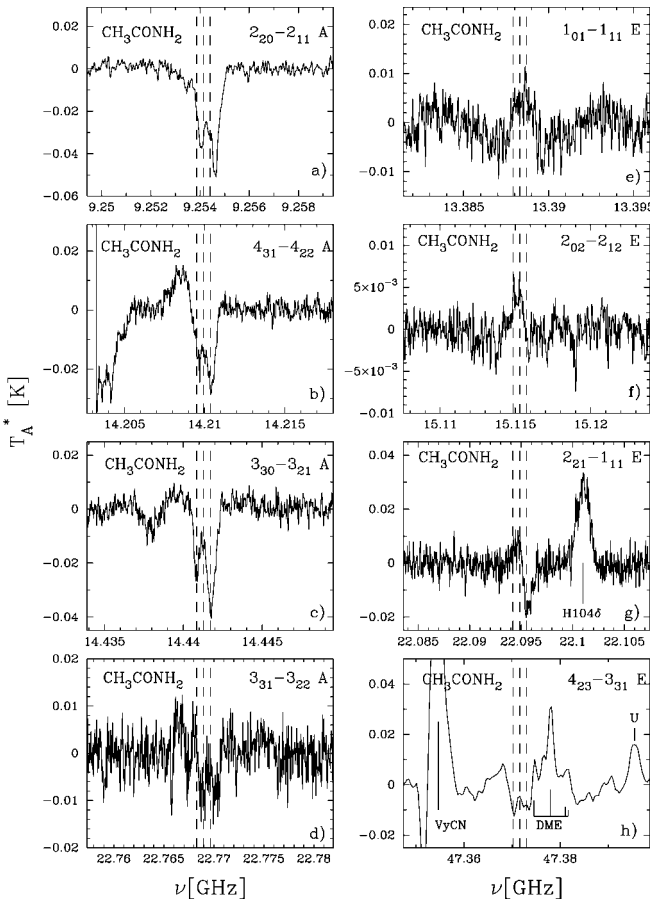

FIG. 3.—Acetamide (CH_3CONH_2) spectra toward Sgr B2(N-LMH) at 24.4 kHz channel spacing (except the 4_{23}–3_{31} *E* is at 390 kHz channel spacing). Same as Fig. 2, except that acetamide hyperfine structure splitting is too small to be resolved in this source. Dashed lines are shown where LSR velocities at +64, +73, and +82 km s^{-1} fall on the frequency axes. Panel *h* shows contaminating lines of vinyl cyanide (VyCN), a dimethyl ether (DME) complex, and an unidentified (U) line at 47.3955 GHz.

ent molecule of acetamide that could be formed from the exothermic neutral-radical reaction of formamide with the methylene radical; shocks associated with the star-forming region could power the reaction to overcome any activation barrier. The abundance ratio of acetamide to formamide is determined to be in the range of ~0.1 to ~0.5 for the cold halo region. The presence of acetamide and formamide in interstellar clouds suggests that these two species could be raw material molecules that are incorporated into comets forming from such clouds. Neither molecule has yet been reported in comets. Formamide and acetamide are the only two known interstellar molecules containing a peptide bond that provides the linkage for the polymerization of amino acids. These molecules are thus of potential biological significance if distributed by comets in protostellar systems.

We thank Karl Irikura for information on reaction energetics, Lew Snyder for useful discussions on radiative transfer, Karl Menten for critical comments, Michael Remijan for programming support and development, and Bill Saxton for the graphic art in Figure 1.

REFERENCES

Allamandola, L. J., Bernstein, M. P., Sandford, S. A., & Walker, R. L. 1999, Space Sci. Rev., 90, 219
Chengalur, J. N., & Kanekar, N. 2003, A&A, 403, L43
Herbst, E. 1995, Ann. Rev. Phys. Chem., 46, 27
Hollis, J. M. 2005, in IAU Symp. 231, Astrochemistry: Recent Successes and Current Challenges, ed. D. Lis, G. Blake, & E. Herbst (Cambridge: Cambridge Univ. Press), 227
Hollis, J. M., Jewell, P. R., Lovas, F. J., & Remijan, A. 2004a, ApJ, 613, L45
Hollis, J. M., Jewell, P. R., Lovas, F. J., Remijan, A., & Møllendal, H. 2004b, ApJ, 610, L21
Hudson, R. L., Moore, M. H., & Gerakines, P. A. 2001, ApJ, 550, 1140
Ilyushin, V. V., Alekseev, E. A., Dyubko, S. F., Kleiner, I., & Hougen, J. T. 2004, J. Mol. Spectrosc., 227, 115
Kojima, T., Yano, E., Nakagawa, K., & Tsunekawa, S. 1987, J. Mol. Spectrosc., 122, 408
Kurland, R. J., & Wilson, E. B., Jr. 1957, J. Chem. Phys., 27, 585
Mehringer, D. M., & Menten, K. M. 1997, ApJ, 474, 346
Moore, M. H., Hudson, R. L., & Gerakines, P. A. 2001, Spectrochim. Acta A, 57, 843
Rubin, R. H., Swenson, G. W., Benson, R. C., Tigelaar, H. L., & Flygare, W. H. 1971, ApJ, 169, L39
Suenram, R. D., Golubiatnikov, G. Yu., Leonov, I. I., Hougen, J. T., Ortigoso, J., Kleiner, I., & Fraser, G. T. 2001, J. Mol. Spectrosc., 208, 188
Taylor, B. N., & Kuyatt, C. E. 1994, NIST Tech. Note 1297 (Washington, DC: US GPO)
Ulich, B. L., & Haas, R. W. 1976, ApJS, 30, 247